Appendix 9. Maps Showing Kriging Estimates and Observations

Maps showing kriging estimates and uncertainties for selected constituents measured for in water samples collected from wells in the Idaho National Laboratory water-quality aquifer monitoring network. Quantile kriging was applied to measured concentrations averaged over the period from 1989 through 2018. The predicted values are back-transformed into concentration space using the midpoint model within a standardized-rank interval of the empirical distribution function (Journel and Deutsch, 1997). Kriging estimates are predicted at points on a regular grid with a spacing of 500 meters and an interpolation domain that is defined by a generalization of the convex hull of the monitoring wells.

The base map was derived from the U.S. Geological Survey National Elevation Dataset 1/3 arc-second digital elevation model. Albers Equal-Area Conic projection using a central meridian of 113°W, standard parallel of 42°50'N and 44°10'N, a false easting of 200,000 meters, and the latitude of the projection's origin at 41°30'N. North American Datum of 1983.

Figures

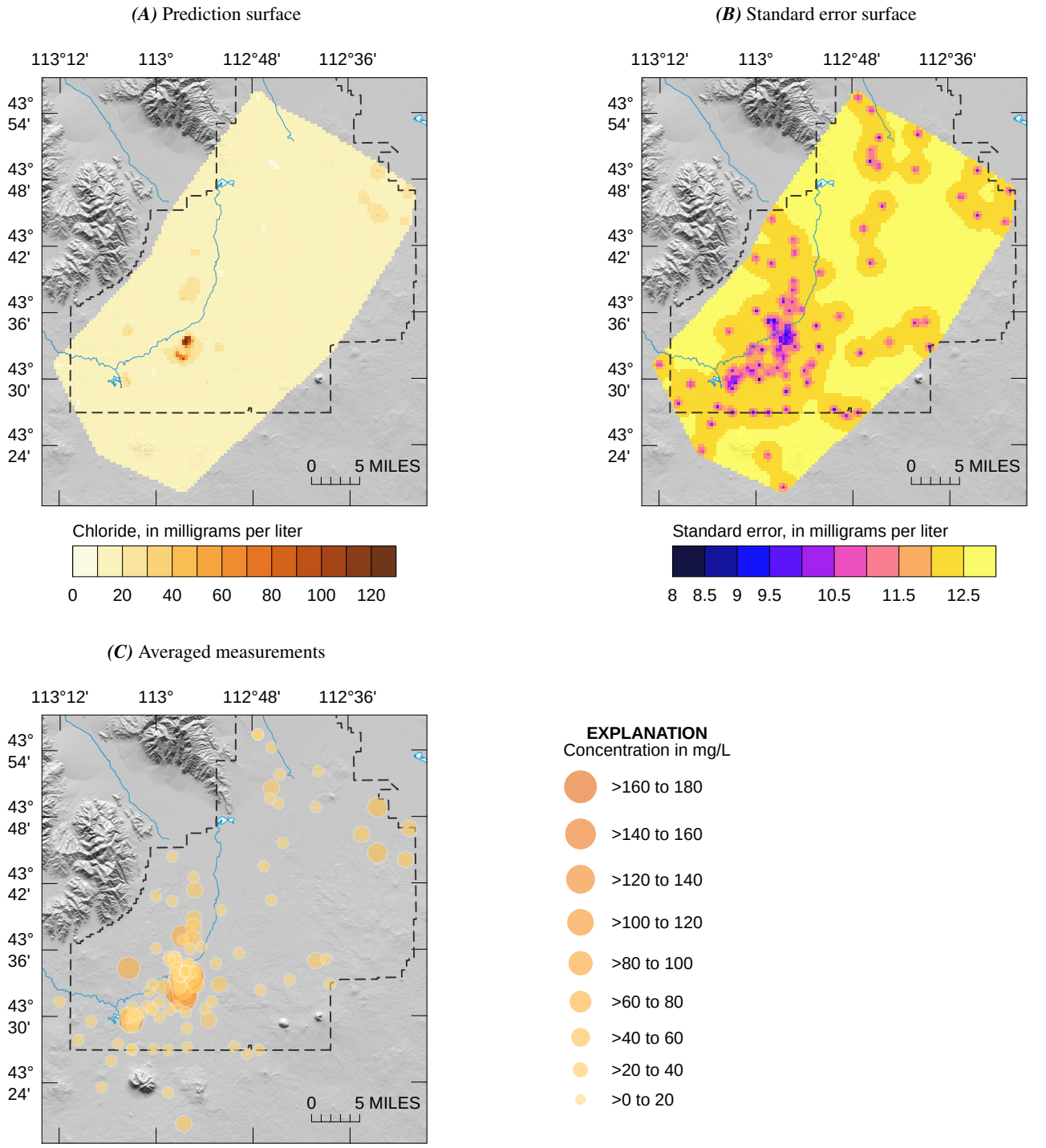

Figure 9.1. Kriging estimates of the (***A***) prediction surface and (***B***) standard error surface, based on (***C***) time- and depth-averaged measurements of chloride concentrations in milligrams per liter (mg/L).

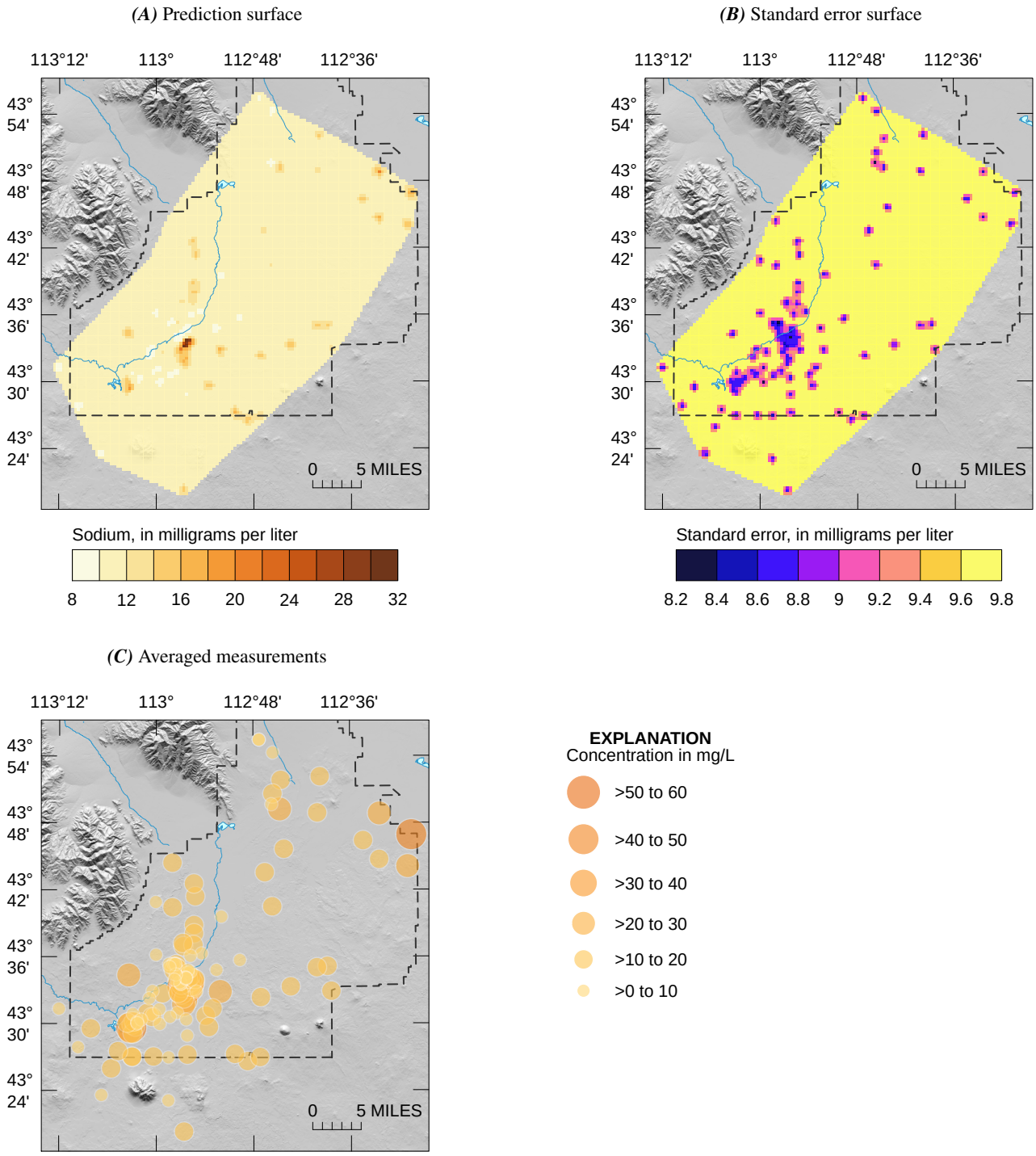

Figure 9.2. Kriging estimates of the (***A***) prediction surface and (***B***) standard error surface, based on (***C***) time- and depth-averaged measurements of sodium concentrations in milligrams per liter (mg/L).

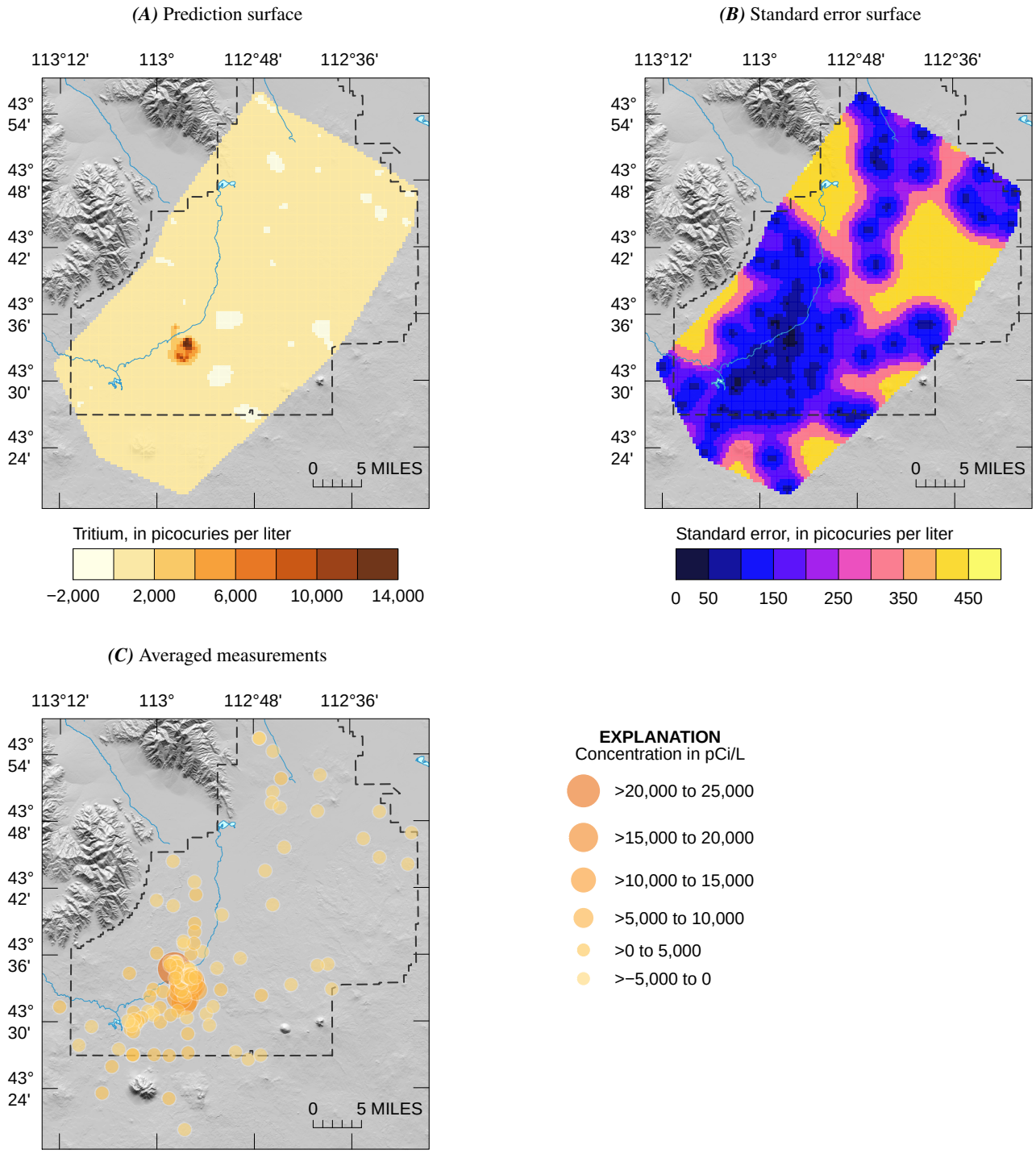

Figure 9.3. Kriging estimates of the (***A***) prediction surface and (***B***) standard error surface, based on (***C***) time- and depth-averaged measurements of tritium concentrations in picocuries per liter (pCi/L).

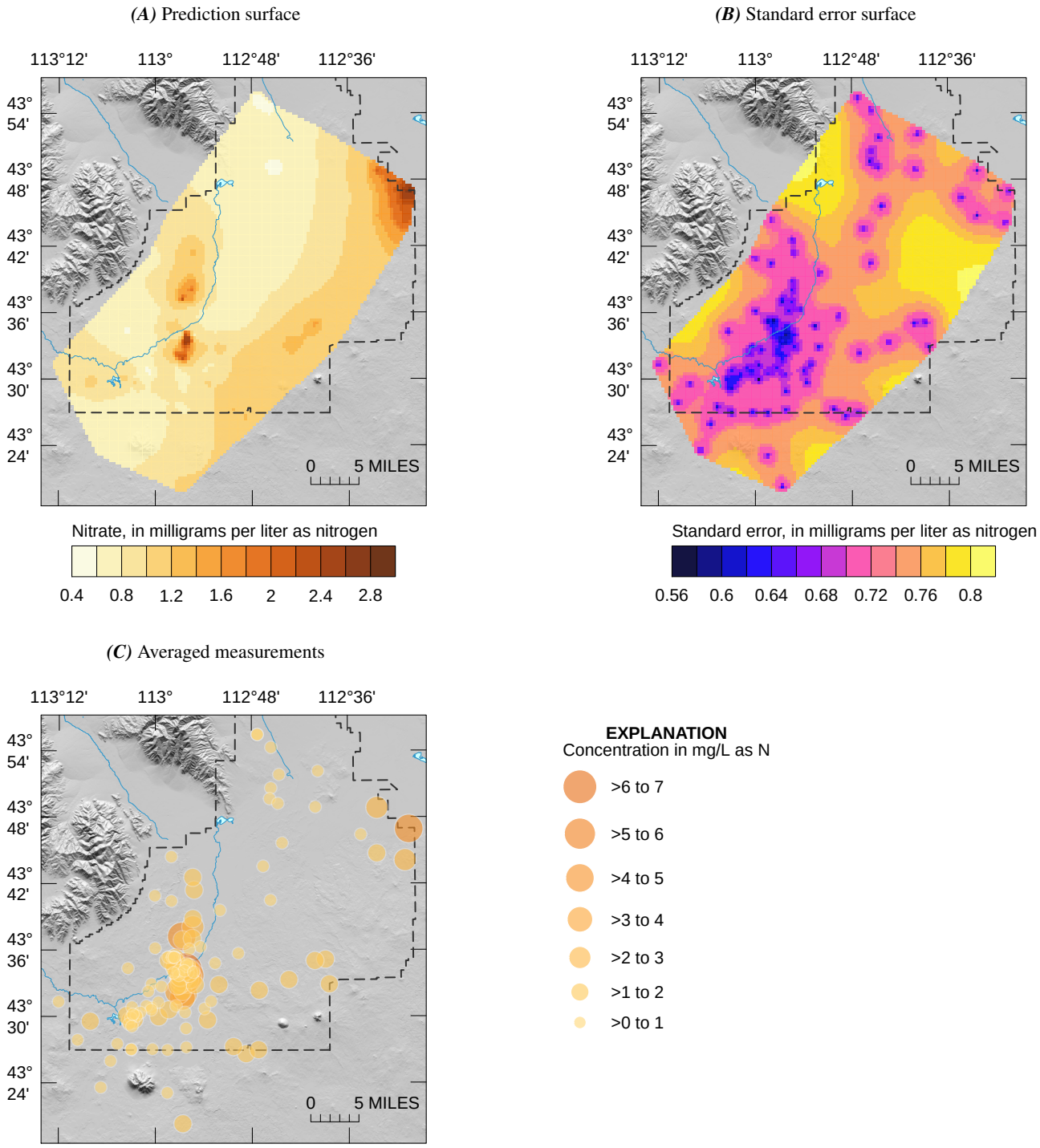

Figure 9.4. Kriging estimates of the (***A***) prediction surface and (***B***) standard error surface, based on (***C***) time- and depth-averaged measurements of nitrate concentrations in milligrams per liter as nitrogen (mg/L as N).

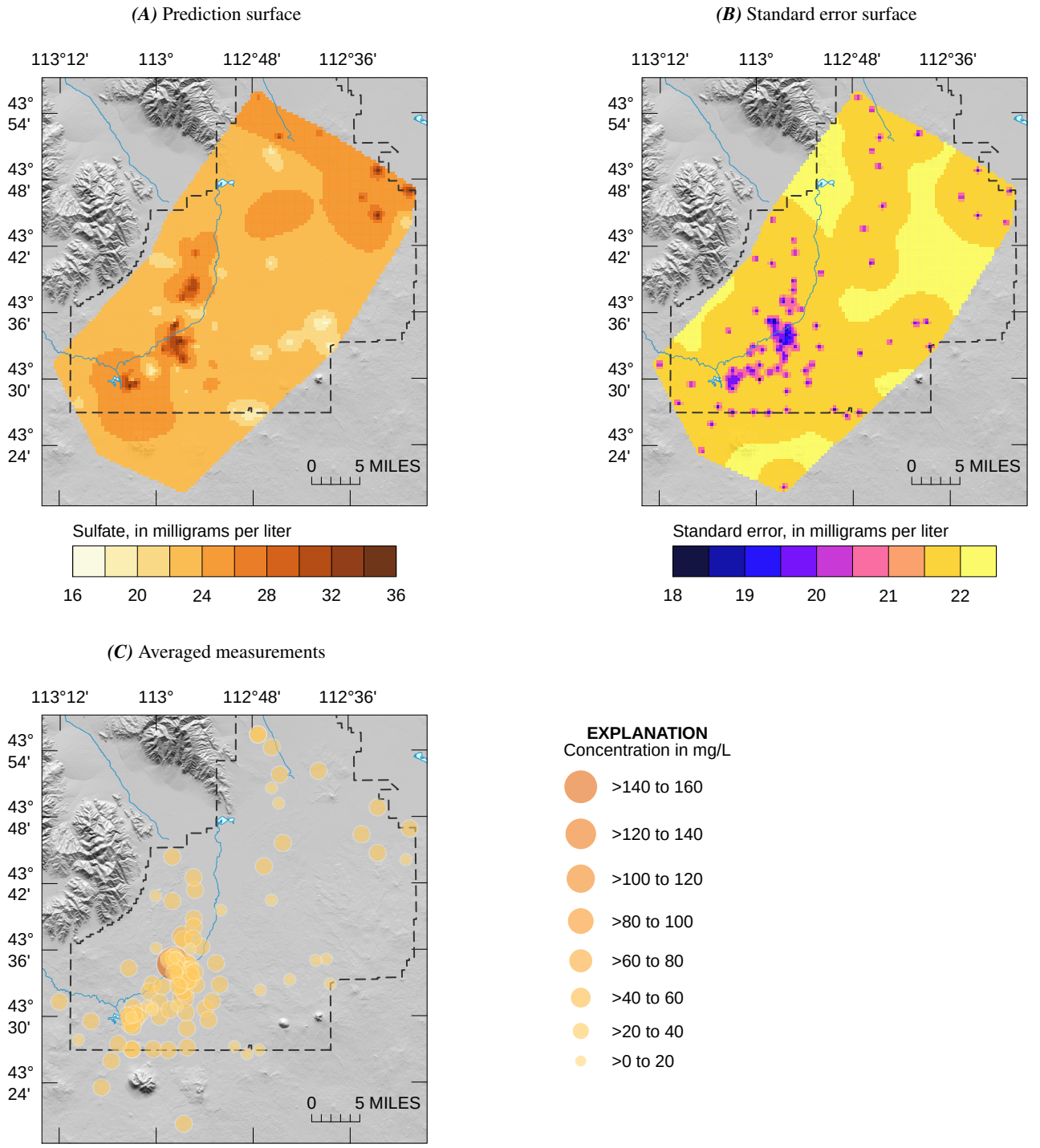

Figure 9.5. Kriging estimates of the (***A***) prediction surface and (***B***) standard error surface, based on (***C***) time- and depth-averaged measurements of sulfate concentrations in milligrams per liter (mg/L).

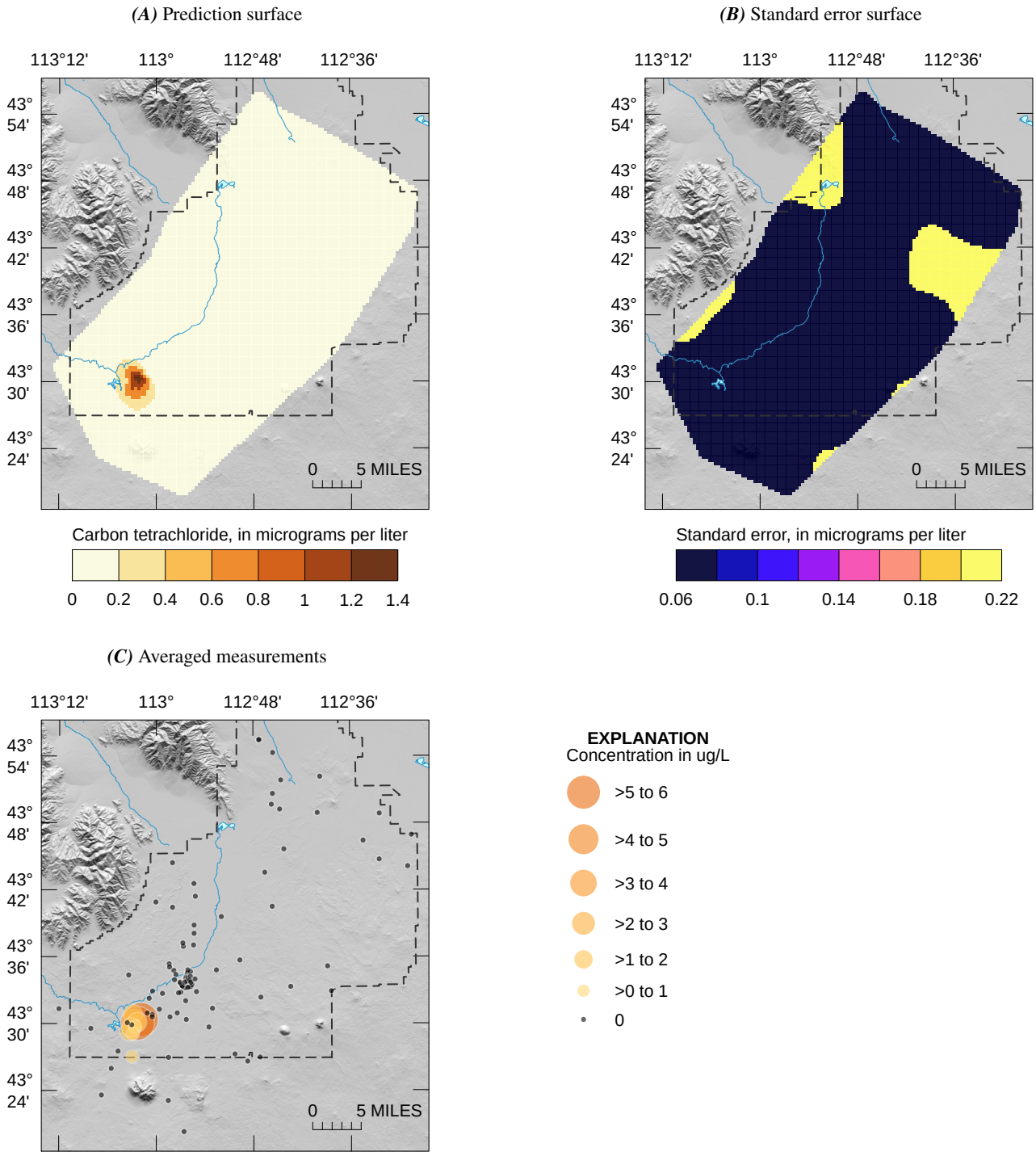

Figure 9.6. Kriging estimates of the (***A***) prediction surface and (***B***) standard error surface, based on (***C***) time- and depth-averaged measurements of carbon tetrachloride concentrations in micrograms per liter (µg/L).

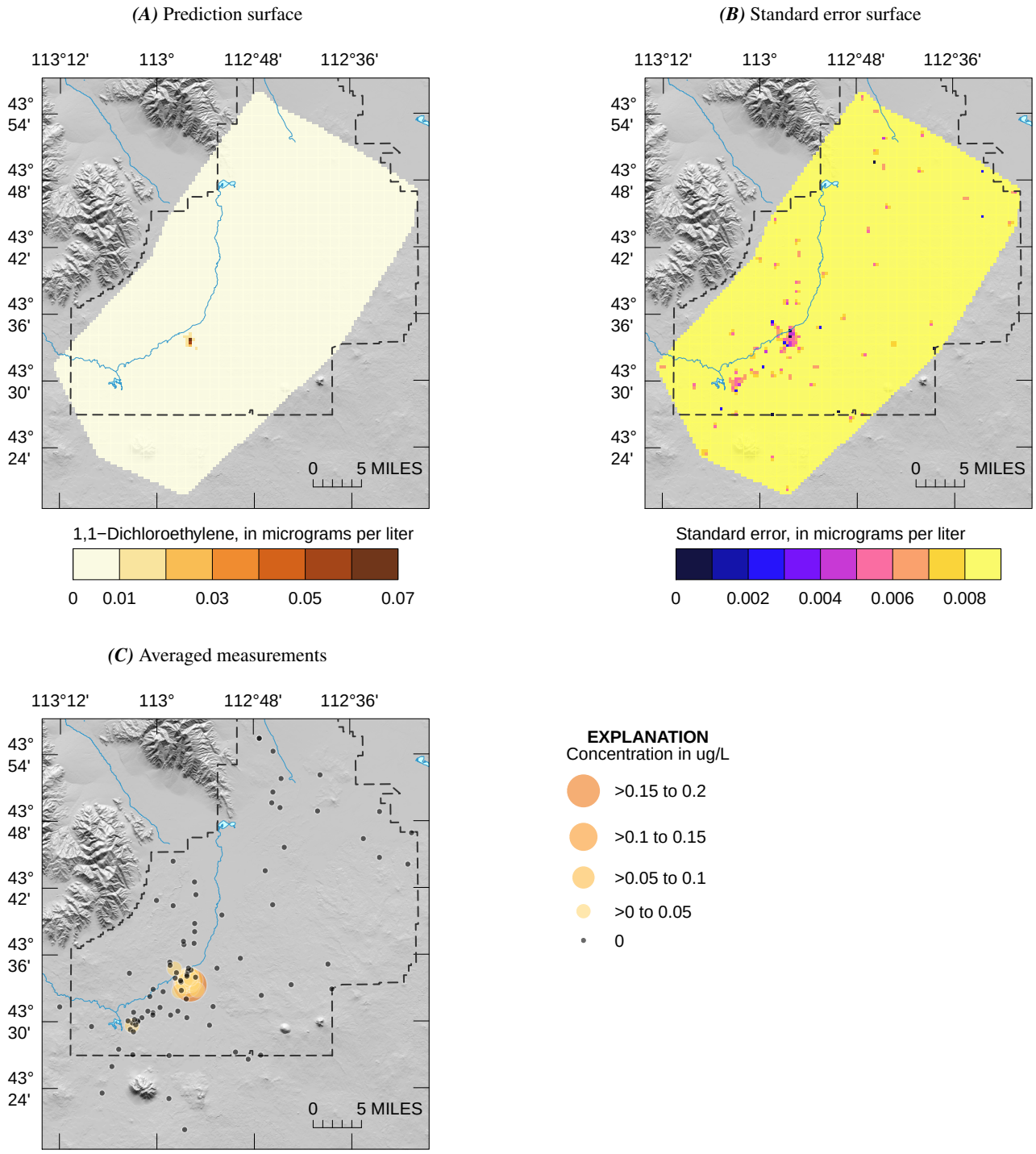

Figure 9.7. Kriging estimates of the (***A***) prediction surface and (***B***) standard error surface, based on (***C***) time- and depth-averaged measurements of 1,1-dichloroethylene concentrations in micrograms per liter (µg/L).

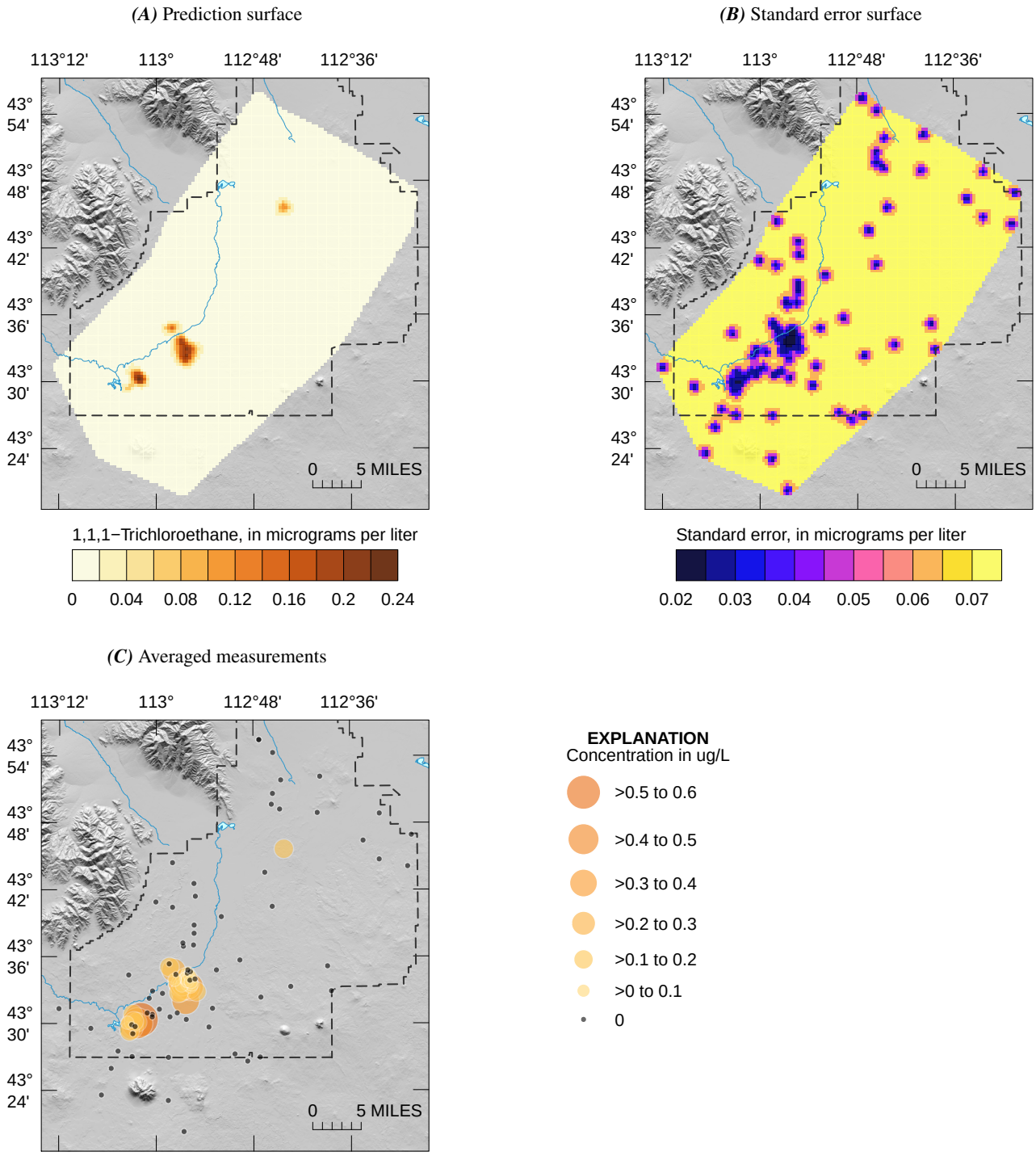

Figure 9.8. Kriging estimates of the (***A***) prediction surface and (***B***) standard error surface, based on (***C***) time- and depth-averaged measurements of 1,1,1-trichloroethane concentrations in micrograms per liter (µg/L).

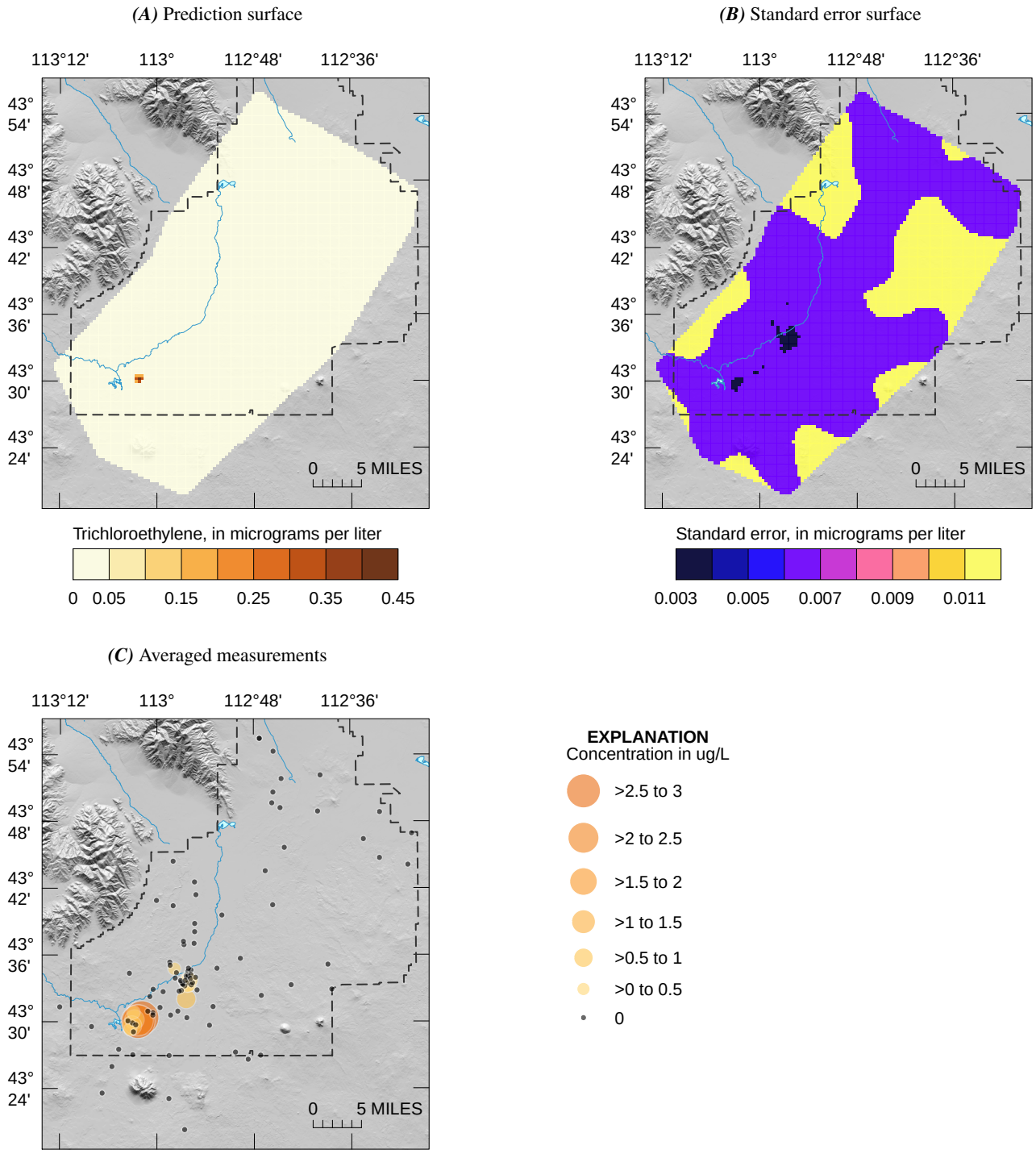

Figure 9.9. Kriging estimates of the (***A***) prediction surface and (***B***) standard error surface, based on (***C***) time- and depth-averaged measurements of trichloroethylene concentrations in micrograms per liter (µg/L).

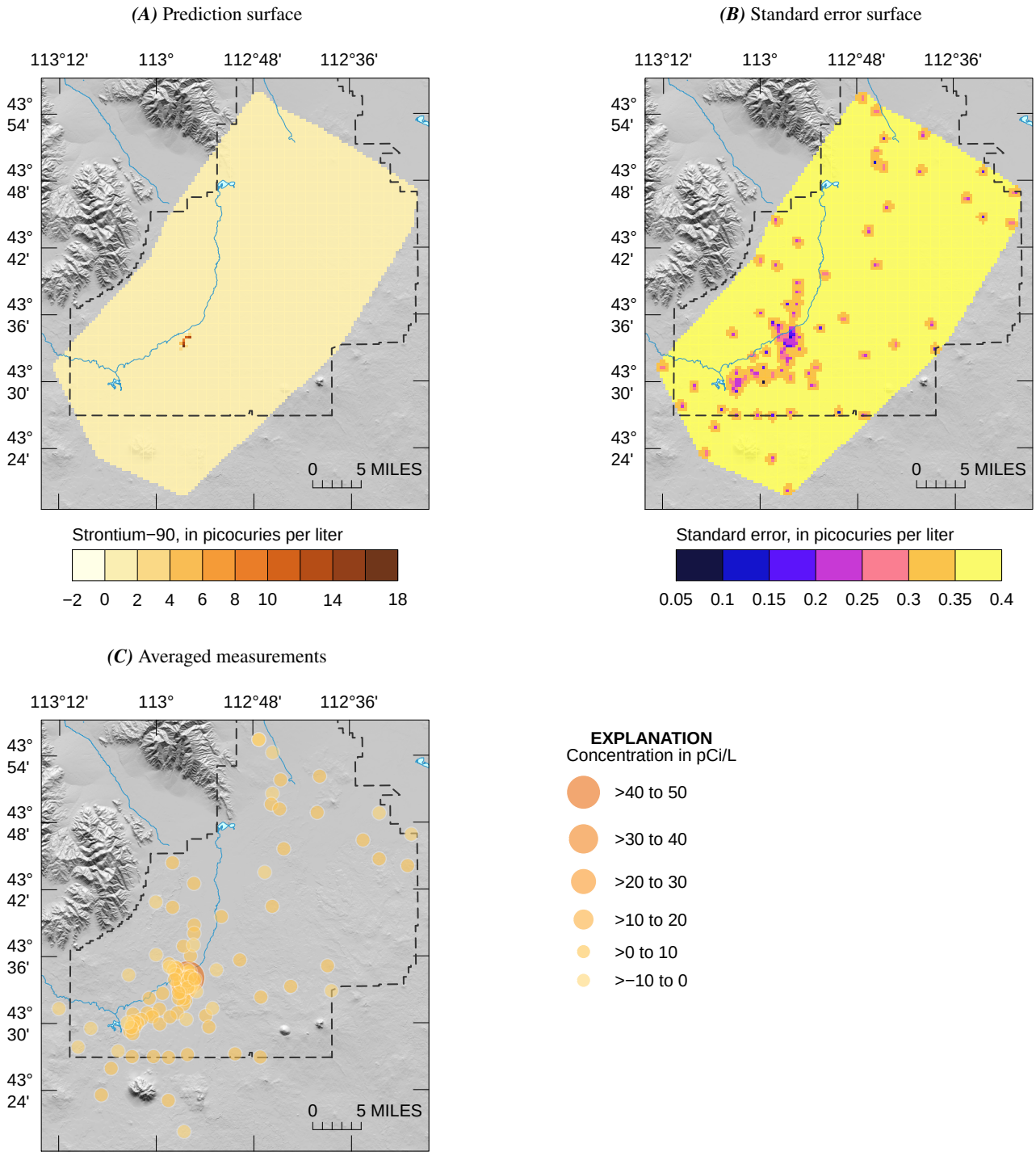

Figure 9.10. Kriging estimates of the (***A***) prediction surface and (***B***) standard error surface, based on (***C***) time- and depth-averaged measurements of strontium-90 concentrations in picocuries per liter (pCi/L).

References Cited

Journel, A.G. and Deutsch, C.V., 1997, Rank order geostatistics: a proposal for a unique coding and common processing of diverse data, in Geostatistics Wollongton '96, ed. by Baafi, E.Y. and Schofield, N.A., vol. 1, Dordrecht, Boston: Kluwer Academic, pp. 174–187.